**High glucose alters the secretome of mechanically stimulated osteocyte-like cells affecting osteoclast precursor recruitment and differentiation**

Marta Maycas[1], María Teresa Portolés[2], María Concepción Matesanz[2], Irene Buendía[3], Javier Linares[4], María José Feito[4], Daniel Arcos[4], María Vallet-Regí[4], Lilian Plotkin[5], Pedro Esbrit[1], and Arancha R. Gortázar[3*].

[1]Laboratorio de Metabolismo Mineral y Óseo, Instituto de Investigación Sanitaria (IIS)-Fundación Jiménez Díaz, UAM, Madrid, Spain;

[2]Departamento de Bioquímica yBiología Molecular I, Facultad de Ciencias Químicas, UCM, Instituto de Investigación Sanitaria San Carlos (IdISSC),Madrid, Spain;

[3] IMMA- Facultad de Medicina, Universidad San Pablo CEU, 28868 Boadilla del Monte, Madrid, Spain;

[4]Departamento de Química Inorgánica y Bioinorgánica, Facultad de Farmacia, UCM, and Instituto de Investigación Sanitaria Hospital 12 de Octubre (i+12) CIBER-BBN, Madrid, Spain;

[5] Department of Anatomy and Cell Biology, Indiana University School of Medicine, and Roudebush Veterans Administration Medical Center, and Indiana Center for Musculoskeleatl Health, Indianapolis, Indiana, USA

To whom all correspondence should be addressed:

Arancha R. Gortázar, PhD,

IMMA-Facultad de Medicina, Universidad San Pablo CEU, Carretera de Boadilla 5,300, 28668 Boadilla del Monte, Madrid, Spain.

E-mail: argortazar@ceu.es

**Running head**: High glucosealters osteocyte-osteoclast communication.

**Key words: Diabetes mellitus; mechanotransduction; osteocyte; osteoclast migration; osteoclastogenesis.**

Total number of figures: 6
Contract grant sponsor: Universidad San Pablo CEU (Emerging Group),
Contract grant sponsor: Ministerio de Ciencia e Innovación; Contract grant number: MAT2012-35556
Contract grant sponsor: Ministerio de Economía y Competitividad; Contract grant number: MAT2013-43299-R
Contract grant sponsor: Agening Network of Excellence; Contract grant number: CSO2010-11384-E.

**ABSTRACT**

Diabetes mellitus (DM) induces bone deterioration, while mechanical stimulation promotes osteocyte-driven bone formation. We aimed to evaluate the interaction of acute exposure (24h) to high glucose (HG) with both the pro-survival effect conferred to osteocytic MLO-Y4 cells and osteoblastic MC3T3-E1 cells by mechanical stimulation and the interaction of these cells with osteoclast precursor RAW264.7 cells. We found that 24h of HG (25 mM) pre-exposure prevented both cell survival and ERK and β-catenin nuclear translocation upon mechanical stimulation by fluid flow (FF) (10 min) in both MLO-Y4 and MC3T3-E1 cells. However, migration of RAW 264.7 cells was inhibited by MLO-Y4 cell-conditioned medium (CM), but not by MC3T3-E1 cell-CM, with HG or FF. This inhibitory effect was associated with consistent changes in VEGF, RANTES, MIP-1α, MIP-1β MCP-1 and GM-CSF in MLO-Y4 cell-CM. RAW264.7 proliferation was inhibited by MLO-Y4 CM under static or HG conditions, but itincreased by FF-CM with or without HG. In addition, both FF and HG abrogated the capacity of RAW 264.7 cells to differentiate into osteoclasts, but in a different manner. Thus, HG-CM in static condition allowed formation of osteoclast-like cells, which were unable to resorb hydroxyapatite. In contrast, FF-CM prevented osteoclastogenesis even in HG condition. Moreover, HG did not affect basal RANKL or IL-6 secretion or their inhibition induced by FF in MLO-Y4 cells. In conclusion, this *in vitro* study demonstrates that HG exerts disparate effects on osteocyte mechanotransduction, and provides a novel mechanism by which DM disturbs skeletal metabolism through altered osteocyte-osteoclast communication**.**

## INTRODUCTION

Diabetes mellitus (DM) is a complex disease with deleterious effects on the skeleton. In fact, both type 1 (T1D) and type 2(T2D) DM are associated with an increased risk of fractures (Carnevale et al., 2004; Yamamoto et al., 2009); although their bone phenotypes are different. Thus, while T2D patients have normal or high bone mineral density (BMD), T1D patients have reduced BMD (Hofbauer et al., 2007; Nicodemus and Folsom, 2001; Vestergaard, 2007). The underlying mechanisms of bone tissue deterioration and fracture risk elevation in DM remain ill- defined. The increase of glucose concentration and advanced glycation end products (AGEs) accumulation present in both types of DM are thought to be responsible for at least some of the features of diabetic osteopathy, such as the inhibition of proliferation and differentiation of bone cell precursors (Botolin and McCabe, 2006; Saito et al., 2006).

Mechanical force is one of the most important inputs that the skeleton receives to regulate bone mass, shape and microarchitecture (Robling and Turner, 2009). The skeleton is able to adapt to an increased load by stimulating bone formation, while skeletal disuse leads to an increased bone resorption (Aguirre et al., 2006; Bikle et al., 2003; Burr et al., 2002). It is now well established that osteocytes are the main mechanosensor cell in bone, regulating both osteoblast and osteoclast function. Osteocytes are long-lived cells, trapped in the bone mineralized matrix and exhibiting cytoplasmic processes inside narrow tunnels called canaliculi. These cell dendrites define an extensive and complex network, which allows an effective communication not only between neighbor osteocytes but also between osteocytes and osteoblasts and osteoclasts located on the bone surface. This strategic position in the bone mineralized matrix and the complexity of the osteocyte process network allows osteocytes to sense changes in bone load, sending signals to osteoblasts and osteoclasts to form or resorb bone (Bellido, 2014; Maycas et al, 2016). Osteocytes are able to control osteoblast function by producing sclerostin, encoded by the SOST gene, which inhibits osteoblast activity through

antagonizing the Wnt/β-catenin pathway (Kamiya et al., 2008; Poole et al., 2005). In addition, osteocytes produce the receptor activator of nuclear factor κB ligand (RANKL) that supports osteoclast differentiation and activity (Nakashima et al., 2011). Lack of mechanical forces induces osteocyte apoptosis, and this event is related to the recruitment and differentiation of osteoclast precursors. In the absence of mechanical stimulation, osteocytes also produce osteoclast signals to stimulate bone resorption (Aguirre et al., 2006; Plotkin et al., 2015). Factors involved in angiogenesis and osteoclast function, such as vascular endothelial growth factor (VEGF) and RANKL, respectively, are known to increase in live osteocytes located close to apoptotic osteocytes, but the underlying mechanisms targeting bone resorption at specific bone sites are still ill-defined (Kennedy et al., 2012).Chemokines are a family of cytokines that provide key signals for recruiting different subpopulations of leukocytes and other cell types in both physiological and pathological situations (Bryant et al, 2015). Some chemokines are expressed by bone cells and could be involved in osteoclast recruitment (Lin et al, 2014; Yu et al, 2004).

Of interest, it has been recently shown that a diabetic environment hampers some downstream responses to mechanical stimulation both *in vivo* and *in vitro* (Parajuli et al., 2015). Therefore, in the present study, we hypothesized that a high glucose (HG) environment might interact with mechanotransduction in MLO-Y4 osteocytes and subsequently with osteoclast recruitment, differentiation and activity, using murine RAW 264.7 monocytic cells as osteoclast precursors.

## MATERIALS AND METHODS

*Cell cultures:* The osteocytic MLO-Y4 cell line, derived from murine long bones(Kato et al., 1997) and MLO-Y4 nuclear-GFP cells, stably transfected with nuclear green fluorescent protein (nGFP) (Plotkin et al., 1999),were grown in α-MEM supplemented with 2.5% fetal

bovine serum (FBS), 2.5% calf serum (CS) and 1% penicillin-streptomycin in 5% $CO_2$ at 37 ºC. Mouse pre-osteoblastic MC3T3-E1 cells (CRL-2593; American Type Culture Collection, Mannasas, VA, USA) were grown in α-MEM supplemented with 10% FBS, 1% penicillin-streptomycin and 2 mM glutamine in 5% $CO_2$at 37 ºC. Murine RAW 264.7 macrophages (Suzuki et al., 2008) were grown in α-MEM supplemented with 10% FBS and 1% penicillin-streptomycin in 5% $CO_2$ at 37 ºC. Both MLO-Y4 and MC3T3-E1 cells were plated at $2x10^4$ cells/$cm^2$ on collagen-coated glass slides (FlexCell, Hillsborough, NC, USA); the next day, fresh medium with high D-glucose (HG) (the α-MEM medium -containing 5.5 mM of D-glucose- was supplemented with the necessary amount of D-glucose to reach a final concentration of 25 mM,) (or high L-glucose as osmotic control) or normal glucose (NG) (5.5 mM) was added for 24 h. Then, cells were submitted or not (static control, SC) to mechanical stress by laminar fluid flow (FF) with a shear stress of 10 dynes/cm2, 8 Hz, for 10 min in a Flexcell® Streamer® shear stress device. The media flowed over the cells was consistently serum-depleted α-MEM in every experimental condition. The concentration used for HG (25 mM) is equivalent to 450 mg/dl a widely used concentration in studies mimicking the diabetic milieu in bonecells (Lozano et al, 2009; Parajuli et al, 2015). The magnitude of the predicted fluid flow-induced shear stress in physiological conditions in osteocytes is estimated to be in the range of 8-30 dynes/cm2. Thus, the regimen used in our study lies within the frame of physiological relevance (Sorkin et al, 2004; Weinbaum et al, 1994). Thereafter, different protocols were carried out depending on the endpoint studied. Thus, for Western blot analysis, protein extracts were obtained immediately after FF. For apoptosis determination, cells were exposed to a pro-apoptotic agent (see below) for an additional 6h.Cells were cultured with fresh medium (α-MEM without serum) for an additional 18 h after FF (or SC) to collect the cell-conditioned medium (CM) in the different experimental groups: CM from SC cells in NG medium; CM from FF-stimulated cells in NG medium; CM from SC cells pre-treated with either HG or L-glucose-containing medium; CM from FF-stimulated cells pre-cultured in HG medium.

*Apoptosis and cell viability determination:* Following FF, MLO-Y4 nuclear-GFP or MC3T3-E1 cells were exposed to the well characterized pro-apoptotic agent etoposide (50 μM) in FBS-depleted medium for 6 h and subsequently were fixed with neutral buffered formalin. Apoptosis was assessed by enumerating nGFP positive MLO-Y4 cells exhibiting chromatin condensation and nuclear fragmentation under a fluorescence microscope, as previously reported (Plotkin et al., 1999). For MC3T3-E1 cell death determination, non-adherent cells were collected and pooled with adherent cells (after gentle trypsinization). Cell death was determined by trypan blue exclusion, calculating the percent of nonviable cells -exhibiting intracellular staining- per total cell number.

*Western blot analysis:* Total cell protein was extracted with 50 mMTris–HCl, pH 7.4, 150 mMNaCl, 1mM EDTA, 1% Triton X-100, 1% sodium deoxycholate, and 0.1% sodium dodecyl sulfate (SDS), supplemented with protease inhibitor cocktail P8340 (Sigma-Aldrich, St. Louis, MO, USA) and phosphatase inhibitor cocktail Set II (Calbiochem, San Diego, CA, USA). Nuclear protein extracts were obtained by using the "Subcellular protein fractionation kit" (Pierce, Rockford, IL, USA), according to the manufacturer's instructions. Protein content was determined by BCA Protein Assay (Thermo Fisher Scientific, Rockford, IL, USA) using bovine serum albumin (BSA) as standard. Protein extracts (25-30 μg) were separated on 10 % polyacrylamide gels in reducing conditions, followed by transfer to nitrocellulose membranes (GE-Amersham, Buckinghamshire, UK). Blots were blocked with 2.5% defatted milk in 0.1% Tween-Tris buffered saline (TBS) or with 5% BSA in 0.1% Tween-TBS, pH 7.4, at room temperature for 1 h, and then probed overnight at 4ºC with the following rabbit polyclonal antibodies: p-GSK3β(Ser9) (Cell Signalling, Beverly, MA, USA) (at 1:500 dilution), β-catenin antibody (Abcam, Cambridge, MA, USA) (at 1:4000 dilution), p-ERK1/2 (Thr202/Tyr204) and ERK1/2 antibody (Cell Signalling) (each at 1:1000 dilution); and the mouse monoclonal antibody GSK3β (Cell Signalling). For loading controls, mouse monoclonal anti-α-tubulin antibody (Sigma-Aldrich) and rabbit polyclonal lamin B1 antibody (Abcam) were used where

appropriate. After incubation with the corresponding secondary horseradish peroxidase-coupled IgG (Santa Cruz Biotechnology), blots were developed with ECL system (GE-Amersham), and band intensities were quantified by densitometry.

*Cytokine determination:* Thechemokinesgranulocyte macrophage colony-stimulated factor (GM-CSF), monocyte chemotactic protein (MCP)-1, macrophage inflammatory protein (MIP)-1α, MIP-1β, regulated on activation, normal T cell expressed and secreted (RANTES), and VEGF, were evaluated in MLO-Y4 cell-CM using the Milliplex system (Merck Millipore, St. Charles, MO, USA) on the Bio-Plex platform (Bio-Rad Laboratories, Hercules, CA, USA). RANKL and IL-6 were evaluated in MLO-Y4 cell-CM using specific mouse ELISA Kits from Abcam and Gen-Probe (Diaclone, Besancon, France), respectively, according to the corresponding manufacturer's instructions. The sensitivity of the assays was 10.9 pg/ml for GM-CSF, 6.7 pg/ml for MCP-1, 7.7 pg/ml for MIP-1α, 11.9 pg/ml forMIP-1β, 2.7 pg/ml for RANTES, 0.3 pg/ml for VEGF, 4 pg/ml for RANKL and 10 pg/ml for IL-6 and their inter assay variation coefficient was <12 %.

*Transwell migration assay:* Migration assay was performed using Costar transwell cell culture chamber inserts (Corning Costar Corporation, Cambridge, MA) with an 8 μm pore size. Briefly, $5 \times 10^4$ RAW 264.7 cells were placed in the upper chamber in 100 μL of serum-freestandard medium containing 20% of each MLO-Y4 (A) or MC3T3-E1 (B) cell-conditioned medium for 6 h. Then, the medium and the upper cell layer were removed with the aid of a cotton swab, and cells on the underside of the transwell were fixed, stained with crystal violet and counted in five randomly selected fields at 200× magnification using the phase contrast microscope.

*Wound healing assay:* RAW 264.7 cells ($5 \times 10^4/cm^2$) were seeded on 6-well plates in α-MEM supplemented with 10% FBS. The day after, a scratch was made across the RAW 264.7 cell layer using a sterile pipette tip. Cells were then washed with phosphate-buffered saline (PBS) and the medium was replaced by serum-free standard medium containing 20% of each

MLO-Y4 cell-CM for 6 h. Cells were thereafter cultured for 8 h to allow cell migration, and migrated cells into the scratch were counted at 200x magnification using a Leica DM6000 phase contrast microscope.

*Osteoclast differentiation on hydroxyapatite disks:* RAW-264.7 cells were seeded on hydroxyapatite disks, prepared as previously described (Matesanz et al., 2014), placed into each well of a 24-well culture plate, at a density of $1x10^4$ cells/$cm^2$ in α-MEM without phenol red and supplemented with 4% FBS. In order to stimulate osteoclast differentiation, 40 ng/ml of mouse RANKL and 25 ng/ml M-CSF were added to the culture medium and cells were cultured for 14 days in the presence of MLO-Y4 cell-CM (20% in standard medium), renewing culture medium every 3 days, as previously reported (Torres-Rodríguez et al., 2016). Subsequently, cells were washed with PBS, harvested using PBS-EDTA for 10 min, and counted in a Neubauer hemocytometer for evaluating cell proliferation. Cell suspensions were then centrifuged at 310g for 10 min and resuspended in fresh medium for the analysis of cell viability. Cell viability was determined by propidium iodide (PI) exclusion and flow cytometry after addition of PI (0.005% in PBS, Sigma-Aldrich) to stain the DNA of dead cells.

*Morphological studies by confocal microscopy:* RAW 264.7 cells grown on hydroxyapatite disks as described above for 14 d were fixed with 3.7% p-formaldehyde in PBS for 10 min, washed with PBS and permeabilized with 0.1% Triton X-100 for 3-5 min. The disks with permeabilized cells were then washed with PBS and pre-incubated with 1% BSA in PBS for 20-30 min. Thereafter, cells were incubated with rhodamine phalloidin (1:40, v/v, Molecular Probes, Eugene, OR, USA) for 20 min to stain F-actin filaments. Samples were then washed with PBS and the cell nuclei were stained with DAPI (4′-6-diamidino-2′-phenylindole; Molecular Probes) at 3 μM in PBS. After staining and washing with PBS, cells were examined using a Leica SP2 confocal laser scanning microscope. Rhodamine fluorescence was excited at 540 nm and measured at 565 nm. DAPI fluorescence was excited at 405 nm and measured at 420–480 nm. The presence of multinucleated cells with F-actin rings was used as indicative of

osteoclast-like cell differentiation. To evaluate the geometry of resorption cavities produced by osteoclast-like cells on the surface of hydroxyapatite disks, cells were detached after 14 d of culture as described above, and subsequently, disks were dehydrated, coated with gold-palladium and examined with a JEOL JSM-6400 scanning electron microscope.

*Statistics:* Data are expressed as mean ± standard deviation (SD) of at least 3 experiments carried out in triplicate. Statistical analysis was performed using GraphPad Prism (GraphPad software, La Jolla, CA, USA). Data were analyzed by Kruskal-Wallis test followed byDunn's test. $p<0.05$ was considered significant.

**RESULTS**

It has been previously demonstrated that the same FF regime used here (10 dynes/cm2; 10 min) exerted a pro-survival effect onosteocyticMLO-Y4 cells, related to β-catenin stabilization and a nuclear ERK translocation (de Castro et al., 2015; Gortázar et al., 2013; Maycas et al., 2015). In the present study, we found that FF induced an increase in p-GSK3β, promoting the stabilization and nuclear increase of β-catenin (Fig 1A); and also induced ERK phosphorylation (p-ERK) and its translocation to the nucleus (Fig 1B). Pre-exposure of MLO-Y4 cells to HG (25 mM) for 24 h inhibited both β-catenin and ERK nuclear translocation induced by FF; although HG did not alter the phosphorylation and subcellular localization of the proteins in SC conditions (Fig. 1A,B). Moreover, we found that this HG exposure –but not L-glucose as osmotic control- of MLO-Y4 cells increased apoptosis induced by etoposide, and reversed the protection induced by FF (Fig. 1C, left). Of note, the difference in osteocyte apoptosis between HG and NG was higher in FF than in SC condition (Fig. 1C, right).Similar findings with respect to protein phosphorylation andsubcellular localization, as well as cell death, were observed in pre-osteoblastic MC3T3-E1 cells (Fig. 2).

We next analyzed the effect of HG and FF on the ability of both cell lines to interact with osteoclast precursors. For this purpose, MLO-Y4 and MC3T3-E1 cells were pre-exposed

to either HG or normal glucose (NG) for 24 h, and cells were then subjected to FF or not (SC), followed by collecting the corresponding CM at 18h. We found that the CM from MLO-Y4 cells pre-exposed to HG inhibited RAW 264.7 cell migration (**Fig. 3A, left).** This inhibition was of the same magnitude as that induced by the CM from FF-stimulated MLO-Y4 cells, independently of pre-exposure or not to HG (**Fig. 3A, left**). Similar results were obtained when RAW 264.7 cell migration was assessed using the wound healing assay (**Fig. 3A, right**). In contrast, MC3T3-E1-cell CMs from any of these experimental conditions failed to significantly affect RAW 264.7 cell migration (**Fig. 3B**).The impact of HG and FF on the secretion of several chemokines by MLO-Y4 cells was next evaluated. Consistent with the aforementioned migration data, both FF and HG were found to inhibit the secreted levels of VEGF, RANTES, MIP-1a, MIP-1b, MCP-1 and GM-CSF (**Fig. 4**). Of note, HG in fact potentiated the inhibitory effect of FF on the secretion of all these chemokines (**Fig. 4**).

We next assessed the effect of the different MLO-Y4 cell-CMs on the viability, proliferation and differentiation of osteoclast precursors after 14 d in osteoclast differentiation medium. First, we observed that none of these CMs tested significantly modified RAW 264.7 cell viability (**Fig. 5A**). On the other hand, the CM from SC cells pre-treated or not with HG (or L-glucose) inhibited RAW 264.7 cell proliferation; whereas the CM from MLO-Y4 cells subjected to FF highly stimulated proliferation, independently of HG pre-exposure or not (**Fig. 5B**). The effect of MLO-Y4 cell-CM on osteoclastogenesis was also analyzed in RAW 264.7 cells after 14 days of culture in the presence of RANKL and M-CSF by the identification of actin rings as a critical feature of mature osteoclasts. The CM from NG-SC osteocytic cells was able to induce osteoclast differentiation, inducing the formation of giant cells with actin rings and at least 3 nuclei, as observed by confocal microscopy **(Fig.5C, upper panel)**.To evaluate the activity of these osteoclast-like cells, we seeded RAW 264.7 cells on hydroxyapatite disks for 14 d in the presence of RANKL/M-CSF and the different MLO-Y4 cell-CMs.CM from cells in SC conditions induced osteoclast activity, as detected by the geometry of resorption cavities

produced by these cells whenexamined by SEM (**Fig. 5C, lower panel, D**). Interestingly, CM from MLO-Y4 cells pre-treated with HG allowed osteoclast-like cell formation but these cells showed minimal resorption activity on hydroxyapatite; whereas CM from FF-stimulated cells decreased osteoclast activity, even in the absence of HG (**Fig. 5C, D**).

Consistent with these findings, RANKL and IL-6 secretion by MLO-Y4 cells were not affected by cell exposure to either HG (or L-glucose) in SC conditions; whereas FF stimulation, following HG pre-exposure or not, decreased the secreted levels of both cytokines (**Fig. 6**).

## DISCUSSION

DM is a metabolic disease characterized by an inappropriate regulation of glucose metabolism affecting a variety of tissues including bone. At the cellular level, HG has been described to: inhibit proliferation and osteogenic differentiation of bone marrow mesenchymal cells; impair osteoblast mineralization; increase osteocyte and osteoblast apoptosis; and inhibit RANKL-induced osteoclastogenesis (Bouillon et al., 1995; Wittrant et al., 2008; Xu et al., 2015). In the present study, we further confirmed that HG prevented the protection conferred by mechanical stimulation by FF to osteoblastic lineage cells. Furthermore, we disclosed a differential impact of FF and HG on osteocyte-osteoclast communication.

Both osteoblasts and osteocytes are able to detect and respond to mechanical and hormonal stimuli, but osteocytes -the main cell type in bone- uniquely coordinate the function of both osteoblasts and osteoclasts. Whereas mechanical loading was found to promote both osteoblast and osteocyte survival (present results and Bin et al, 2016; Maycas et al, 2016),only dying osteocytes (not osteoblasts) induce osteoclastogenesis (Kogianni et al, 2008).In this study, we aimed to explore the putative effect of HG on osteocyte-osteoclast communication, and we also used an osteoblastic cell line, MC3T3-E1 cells, to confirm the specificity of the observed effects of the CM from osteocytic MLO-Y4 cells on the migration of osteoclast precursors. As

shown in fig 3, as expected, only the CM from osteocytic MLO-Y4 but not that from osteoblastic MC3T3-E1 cells modulated osteoclast precursor migration, confirming the important role of osteocytes in osteoclast function.

A very recent study has shown that the anabolic effect induced by bone loading was impaired in a T1D mouse model (Parajuli et al., 2015). These authors also showed that some of the beneficial effects induced by FF in MLO-Y4 cells, namely the inhibition of caspase 3/7 expression and induction of prostaglandin E2, were compromised by HG exposure. In the same line, we here found that cell survival, and two related mechanistic events -β-catenin and ERK nuclear translocation- induced by mechanical stimulation in MLO-Y4 cells were dramatically decreased by HG exposure. In the aforementioned study, HG exposure was also found to reverse the reduction of RANKL secretion induced by FF, in contrast to the present data. This difference between the two studies could be explained by the different pattern of treatments: whereas we exposed MLO-Y4 cells to HG for 24 h followed by 10 min FF, in the report by Parajuli et al.(2015), MLO-Y4 cells were incubated with HG for 72 h prior to FF for 2 h. Indeed, the impact of HG on osteoblastic cells depends on time of exposure (Botolin et al, 2006; López-Herradón et al, 2013). In the present study, we observed that an acute exposure of MLO-Y4 cells to HG (24 h) prevented both ERK and β-catenin relocalization but only after mechanical stimulation by FF and not under SC conditions. Thus, this time of HG exposure does not seem to be sufficient to affect the basal levels of both proteins, although it might affect the formation of other components of the signalsome triggered by mechanotransduction leading to ERK and beta-catenin relocalization (Plotkin et al, 2005; Gortázar et al., 2013). In this regard, α5-integrin, which is required for osteocyte mechanotransduction (Plotkin et al, 2005), has recently been shown to be reduced by HG in fibroblastic cells (Almeida et al, 2016).

In the present study, the secretion of various chemokines, namely VEGF, RANTES, MIP-1α, MIP-1β, MCP-1 and GM-CSF, was found to be inhibited following mechanical stimulation of MLO-Y4 cells by FF. This inhibitory effect was recapitulated -or even

potentiated- by HG pre-exposure of these cells. Accordingly, RAW 264.7 cell migration in the presence of CM from these osteocytic cells after FF or HG treatment was also inhibited compared to that observed with the CM from the corresponding non-mechanically stimulated cells.

Inhibition of cell proliferation and arrest of cell cycle progression are required for osteoclast differentiation. RANKL has been reported to suppress proliferation of osteoclastic cells (Bharti et al., 2004) through induction of the cyclin-dependent kinase inhibitors p27KIP1 and p21CIP1 (Sankar et al., 2004). According to this notion, we found that exposure of RAW 264.7 cells to the MLO-Y4-cell CM inhibited their proliferation but allowed osteoclast-like cell formation, while the opposite occurred after exposure to the CM of FF-stimulated cells independently of the presence of HG. Consistently, this mechanical stimulation reduced the production of RANKL by these osteocytic cells, as shown here and previously by other investigators (Kim et al., 2006; Lau et al., 2010). In this sense, we also found that IL-6 secretion was inhibited by FF. This cytokine has been shown to promote bone resorption mainly by its ability to increase RANKL production in osteoblastic lineage cells (Palmqvist et al., 2002; Tamura et al., 1993). Moreover, IL-6 is able to stimulate osteoclast formation *in vitro*, and IL-6 receptors have been identified in mature osteoclasts (Gao et al., 1998; Tamura et al., 1993). Furthermore, it isknown that mechanical stimulation of osteocytes induces the production of other factors that caninhibit osteoclast differentiation, such as nitric oxide or the phosphoglycoprotein MEPE (Kulkarni et al., 2010; Tan et al., 2007). Our results also showed that FF or HG pre-treatment of MLO-Y4 cells had a different consequence on osteoclast function. Thus, in contrast to FF, HG pre-exposure failed to affect either RANKL or IL-6 secretion and allowed the formation of osteoclast multinucleated giant cells, although they were unable to resorb hydroxyapatite. The effect of DM on osteoclastogenesis and osteoclast activity *in vivo* is presently unclear (Bouillon et al., 1995; McCabe, 2007; Tsentidis et al., 2015), but osteoclast precursor exposure to HG in vitro has been shown to directly inhibit the expression of

two molecules, v-ATPase V0 subunit d2 and dendritic cell-specific transmembrane protein, which are key in the process of osteoclast fusion (Wittrant et al., 2008; Xu et al., 2015). Collectively, these data suggest that HG might directly and indirectly inhibit osteoclast function, affecting the formation of mature osteoclasts from osteoclast progenitors and also osteoclast activity by targeting osteocytes.

The present findings are the first to our knowledge suggesting that HG affects osteocyte mechanotransduction to impact osteocyte-osteoclast communication, and open new avenues for understanding the mechanisms whereby DM can disturb bone metabolism.

**Acknowledgements:** This study was supported by research grants from Universidad San Pablo CEU (Emerging Group), Ministerio de Ciencia e Innovación (MAT2012-35556), Ministerio de Economía y Competitividad (MAT2013-43299-R) and Agening Network of Excellence (CSO2010-11384-E). M.Maycas(FI12/00458) and M.C. Matesanzwere supported by Spanish Ministerio de Economía y Competitividad. We wish to thank Dr. Lynda Bonewald, (University of Missouri, Kansas City, MO, USA) and Dr.Teresita Bellido (University of Indiana, Indianapolis, IN, USA) for kindly supplying MLO-Y4 and MLO-Y4-nGFP cells, respectively. We are also indebted to the staff of the ICTS-Centro Nacional de Microscopía Electrónica and Centro de Citometría y Microscopía de Fluorescencia of UCM (Madrid,Spain) for assistance in scanning electron microscopy and flow cytometry studies, respectively. We are thankful to Mark S. Davis for proofreading the manuscript.

## LITERATURE CITED

Aguirre, J.I., Plotkin, L.I., Stewart, S.A., Weinstein, R.S., Parfitt, A.M., Manolagas, S.C., Bellido, T., 2006. Osteocyte apoptosis is induced by weightlessness in mice and precedes osteoclast recruitment and bone loss. J. Bone Miner. Res. 21, 605–615. doi:10.1359/jbmr.060107

Almeida, M.E., Monteiro K.S., Kato E.E., Sampaio S.C., Braga T.T., Câmara N.O., Lamers M.L., Santos M.F., 2016.Hyperglycemia reduces integrin subunits alpha v and alpha 5 on the surface of dermal fibroblasts contributing to deficient migration.Mol Cell Biochem. 421:19-28.

Bellido, T., 2014. Osteocyte-driven bone remodeling. Calcif. Tissue Int. 94, 25–34. doi:10.1007/s00223-013-9774-y

Bharti, A.C., Takada, Y., Shishodia, S., Aggarwal, B.B., 2004. Evidence that receptor activator of nuclear factor (NF)-kappaB ligand can suppress cell proliferation and induce apoptosis through activation of a NF-kappaB-independent and TRAF6-dependent mechanism. J. Biol. Chem. 279, 6065–6076. doi:10.1074/jbc.M308062200

Bikle, D.D., Sakata, T., Halloran, B.P., 2003. The impact of skeletal unloading on bone formation. Gravitational Space Biol. Bull. Publ. Am. Soc. Gravitational Space Biol. 16, 45–54.

Bin G., Bo Z., Jing W., Jin J., Xiaoyi T., Cong C., Liping A., Jinglin M., Cuifang W., Yonggang C., Yayi X., 2016. Fluid shear stress suppresses TNF-α-induced apoptosis in MC3T3-E1 cells: Involvement of ERK5-AKT-FoxO3a-Bim/FasL signaling pathways. Exp Cell Res. 343:208-17.

Botolin, S., McCabe, L.R., 2006. Chronic hyperglycemia modulates osteoblast gene expression through osmotic and non-osmotic pathways. J. Cell. Biochem. 99, 411–424. doi:10.1002/jcb.20842

Bouillon, R., Bex, M., Van Herck, E., Laureys, J., Dooms, L., Lesaffre, E., Ravussin, E., 1995. Influence of age, sex, and insulin on osteoblast function: osteoblast dysfunction in diabetes mellitus. J. Clin. Endocrinol. Metab. 80, 1194–1202. doi:10.1210/jcem.80.4.7714089

Bryant V.L., Slade C.A., 2015. Chemokines, their receptors and human disease: the good, the bad and the itchy Immunol Cell Biol. 93(4):364-71.

Burr, D.B., Robling, A.G., Turner, C.H., 2002. Effects of biomechanical stress on bones in animals. Bone 30, 781–786. doi:10.1016/S8756-3282(02)00707-X

Carnevale, V., Romagnoli, E., D'Erasmo, E., 2004. Skeletal involvement in patients with diabetes mellitus. Diabetes Metab. Res. Rev. 20, 196–204. doi:10.1002/dmrr.449

de Castro, L.F., Maycas, M., Bravo, B., Esbrit, P., Gortazar, A., 2015. VEGF Receptor 2 (VEGFR2) Activation Is Essential for Osteocyte Survival Induced by Mechanotransduction. J. Cell. Physiol. 230, 278–285. doi:10.1002/jcp.24734

Gao, Y., Morita, I., Maruo, N., Kubota, T., Murota, S., Aso, T., 1998. Expression of IL-6 receptor and GP130 in mouse bone marrow cells during osteoclast differentiation. Bone 22, 487–493.

Gortazar, A.R., Martin-Millan, M., Bravo, B., Plotkin, L.I., Bellido, T., 2013. Crosstalk between Caveolin-1/Extracellular Signal-regulated Kinase (ERK) and β-Catenin Survival Pathways in Osteocyte Mechanotransduction. J. Biol. Chem. 288, 8168–8175. doi:10.1074/jbc.M112.437921

Hofbauer, L.C., Brueck, C.C., Singh, S.K., Dobnig, H., 2007. Osteoporosis in Patients With Diabetes Mellitus. J. Bone Miner. Res. 22, 1317–1328. doi:10.1359/jbmr.070510

Kamiya, N., Ye, L., Kobayashi, T., Mochida, Y., Yamauchi, M., Kronenberg, H.M., Feng, J.Q., Mishina, Y., 2008. BMP signaling negatively regulates bone mass through sclerostin by inhibiting the canonical Wnt pathway. Development 135, 3801–3811. doi:10.1242/dev.025825

Kato, Y., Windle, J.J., Koop, B.A., Mundy, G.R., Bonewald, L.F., 1997. Establishment of an Osteocyte-like Cell Line, MLO-Y4. J. Bone Miner. Res. 12, 2014–2023. doi:10.1359/jbmr.1997.12.12.2014

Kennedy, O.D., Herman, B.C., Laudier, D.M., Majeska, R.J., Sun, H.B., Schaffler, M.B., 2012. Activation of resorption in fatigue-loaded bone involves both apoptosis and active pro-osteoclastogenic signaling by distinct osteocyte populations. Bone 50, 1115–1122. doi:10.1016/j.bone.2012.01.025

Kim, C.H., You, L., Yellowley, C.E., Jacobs, C.R., 2006. Oscillatory fluid flow-induced shear stress decreases osteoclastogenesis through RANKL and OPG signaling. Bone 39, 1043–1047. doi:10.1016/j.bone.2006.05.017

Kogianni G., Mann V., Noble B.S., 2008. Apoptotic bodies convey activity capable of initiating osteoclastogenesis and localized bone destruction. J Bone Miner Res;23:915-27.

Kulkarni, R.N., Bakker, A.D., Everts, V., Klein-Nulend, J., 2010. Inhibition of Osteoclastogenesis by Mechanically Loaded Osteocytes: Involvement of MEPE. Calcif. Tissue Int. 87, 461–468. doi:10.1007/s00223-010-9407-7

Lau, E., Al-Dujaili, S., Guenther, A., Liu, D., Wang, L., You, L., 2010. Effect of low-magnitude, high-frequency vibration on osteocytes in the regulation of osteoclasts. Bone 46, 1508–1515. doi:10.1016/j.bone.2010.02.031

Lin T.H., Tamaki Y., Pajarinen J., Waters H.A., Woo D.K., Yao Z., Goodman S.B., 2014. Chronic inflammation in biomaterial-induced periprosthetic osteolysis: NF-κB as a therapeutic target. Acta Biomater ;10:1-10.

López-Herradón A., Portal-Núñez S., García-Martín A., Lozano D., Pérez-Martínez F.C., Ceña V., Esbrit P., 2013.Inhibition of the canonical Wnt pathway by high glucose can be reversed by parathyroid hormone-related protein in osteoblastic cells. J Cell Biochem.;114:1908-16

Lozano D., de Castro L.F., Dapía S., Andrade-Zapata I., Manzarbeitia F., Alvarez-Arroyo M.V., Gómez-Barrena E., Esbrit P. Role of parathyroid hormone-related protein in the decreased osteoblast function in diabetes-related osteopenia. Endocrinology. 2009 May;150(5):2027–35.

Matesanz, M.C., Linares, J., Lilue, I., Sánchez-Salcedo, S., Feito, M.J., Arcos, D., Vallet-Regí, M., Portolés, M.T., 2014. Nanocrystalline silicon substituted hydroxyapatite effects on osteoclast differentiation and resorptive activity. J. Mater. Chem. B 2, 2910–2919. doi:10.1039/C3TB21697G

Maycas, M., Ardura, J.A., de Castro, L.F., Bravo, B., Gortázar, A.R., Esbrit, P., 2015. Role of the Parathyroid Hormone Type 1 Receptor (PTH1R) as a Mechanosensor in Osteocyte Survival. J. Bone Miner. Res. 30, 1231–1244. doi:10.1002/jbmr.2439

Maycas M., Esbrit P., Gortázar A.R., 2016. Molecular mechanisms in bone mechanotransduction. Histol Histopathol. 2016 Dec 16:11858.

McCabe, L.R., 2007. Understanding the pathology and mechanisms of type I diabetic bone loss. J. Cell. Biochem. 102, 1343–1357. doi:10.1002/jcb.21573

Nakashima, T., Hayashi, M., Fukunaga, T., Kurata, K., Oh-hora, M., Feng, J.Q., Bonewald, L.F., Kodama, T., Wutz, A., Wagner, E.F., Penninger, J.M., Takayanagi, H., 2011. Evidence for osteocyte regulation of bone homeostasis through RANKL expression. Nat. Med. 17, 1231–1234. doi:10.1038/nm.2452

Nicodemus, K.K., Folsom, A.R., 2001. Type 1 and Type 2 Diabetes and Incident Hip Fractures in Postmenopausal Women. Diabetes Care 24, 1192–1197. doi:10.2337/diacare.24.7.1192

Palmqvist, P., Persson, E., Conaway, H.H., Lerner, U.H., 2002. IL-6, leukemia inhibitory factor, and oncostatin M stimulate bone resorption and regulate the expression of receptor activator of NF-kappa B ligand, osteoprotegerin, and receptor activator of NF-kappa B in mouse calvariae. J. Immunol. Baltim. Md 1950 169, 3353–3362.

Parajuli, A., Liu, C., Li, W., Gu, X., Lai, X., Pei, S., Price, C., You, L., Lu, X.L., Wang, L., 2015. Bone's responses to mechanical loading are impaired in type 1 diabetes. Bone 81, 152–160. doi:10.1016/j.bone.2015.07.012

Plotkin, L.I., Gortazar, A.R., Davis, H.M., Condon, K.W., Gabilondo, H., Maycas, M., Allen, M.R., Bellido, T., 2015. Inhibition of osteocyte apoptosis prevents the increase in osteocytic receptor activator of nuclear factor κB ligand (RANKL) but does not stop bone resorption or the loss of bone induced by unloading. J. Biol. Chem. 290, 18934–18942. doi:10.1074/jbc.M115.642090

Plotkin L.I., Mathov I., Aguirre J.I., Parfitt A.M., Manolagas S.C., Bellido T.,2005. Mechanical stimulation prevents osteocyte apoptosis: requirement of integrins, Src kinases, and ERKs. Am J Physiol Cell Physiol,289:C633-43.

Plotkin, L.I., Weinstein, R.S., Parfitt, A.M., Roberson, P.K., Manolagas, S.C., Bellido, T., 1999. Prevention of osteocyte and osteoblast apoptosis by bisphosphonates and calcitonin. J. Clin. Invest. 104, 1363–1374. doi:10.1172/JCI6800

Poole, K.E.S., Bezooijen, R.L. van, Loveridge, N., Hamersma, H., Papapoulos, S.E., Löwik, C.W., Reeve, J., 2005. Sclerostin is a delayed secreted product of osteocytes that inhibits bone formation. FASEB J. doi:10.1096/fj.05-4221fje

Robling, A.G., Turner, C.H., 2009. Mechanical signaling for bone modeling and remodeling. Crit. Rev. Eukaryot. Gene Expr. 19, 319–338.

Saito, M., Fujii, K., Mori, Y., Marumo, K., 2006. Role of collagen enzymatic and glycation induced cross-links as a determinant of bone quality in spontaneously diabetic WBN/Kob rats. Osteoporos. Int. 17, 1514–1523. doi:10.1007/s00198-006-0155-5

Sankar, U., Patel, K., Rosol, T.J., Ostrowski, M.C., 2004. RANKL coordinates cell cycle withdrawal and differentiation in osteoclasts through the cyclin-dependent kinase inhibitors p27KIP1 and p21CIP1. J. Bone Miner. Res. 19, 1339–1348. doi:10.1359/JBMR.040321

Sorkin, A.M., Dee, K.C., and Knothe Tate, M.L. (2004). “Culture shock” from the bone cell’s perspective: emulating physiological conditions for mechanobiological investigations. Am. J.Physiol. Cell Physiol. 287, C1527–C1536.

Suzuki, N., Yoshimura, Y., Deyama, Y., Suzuki, K., Kitagawa, Y., 2008. Mechanical stress directly suppresses osteoclast differentiation in RAW264.7 cells. Int. J. Mol. Med. doi:10.3892/ijmm.21.3.291

Tamura, T., Udagawa, N., Takahashi, N., Miyaura, C., Tanaka, S., Yamada, Y., Koishihara, Y., Ohsugi, Y., Kumaki, K., Taga, T., 1993. Soluble interleukin-6 receptor triggers osteoclast formation by interleukin 6. Proc. Natl. Acad. Sci. U. S. A. 90, 11924–11928.

Tan, S.D., de Vries, T.J., Kuijpers-Jagtman, A.M., Semeins, C.M., Everts, V., Klein-Nulend, J., 2007. Osteocytes subjected to fluid flow inhibit osteoclast formation and bone resorption. Bone 41, 745–751. doi:10.1016/j.bone.2007.07.019

Torres-Rodríguez, C., Portolés, M.T., Matesanz, M.C., Linares, J., Feito, M.J., Izquierdo-Barba, I., Esbrit, P., Vallet-Regí, M., 2016. Effects of bleaching on osteoclast activity and their modulation by osteostatin and fibroblast growth factor 2. J. Colloid Interface Sci. 461, 285–291. doi:10.1016/j.jcis.2015.09.035

Tsentidis, C., Gourgiotis, D., Kossiva, L., Doulgeraki, A., Marmarinos, A., Galli-Tsinopoulou, A., Karavanaki, K., 2015. Higher levels of s-RANKL and osteoprotegerin in children and adolescents with type 1 diabetes mellitus may indicate increased osteoclast signaling and predisposition to lower bone mass: a multivariate cross-sectional analysis. Osteoporos. Int. doi:10.1007/s00198-015-3422-5

Vestergaard, P., 2007. Discrepancies in bone mineral density and fracture risk in patients with type 1 and type 2 diabetes- a meta-analysis. Osteoporos. Int.18, 427–444. doi:10.1007/s00198-006-0253-4

Weinbaum, S., Cowin, S.C., and Zeng, Y. (1994). A model for the excitation of osteocytes by mechanical loading-induced bone fluid shear stresses. J. Biomech. 27, 339–360.

Wittrant, Y., Gorin, Y., Woodruff, K., Horn, D., Abboud, H.E., Mohan, S., Abboud-Werner, S.L., 2008. High d(+)glucose concentration inhibits RANKL-induced osteoclastogenesis. Bone 42, 1122–1130. doi:10.1016/j.bone.2008.02.006

Xu, J., Yue, F., Wang, J., Chen, L., Qi, W., 2015. High glucose inhibits receptor activator of nuclear factor-κB ligand-induced osteoclast differentiation via downregulation of v-

ATPase V0 subunit d2 and dendritic cell-specific transmembrane protein. Mol. Med. Rep. 11, 865–870. doi:10.3892/mmr.2014.2807

Yamamoto, M., Yamaguchi, T., Yamauchi, M., Kaji, H., Sugimoto, T., 2009. Diabetic Patients Have an Increased Risk of Vertebral Fractures Independent of BMD or Diabetic Complications. J. Bone Miner. Res. 24, 702–709. doi:10.1359/jbmr.081207

Yu X., Huang Y., Collin-Osdoby P., and Osdoby P., 2004. CCR1 Chemokines Promote the Chemotactic Recruitment, RANKLDevelopment, and Motility of Osteoclasts and Are Induced by inflammatory Cytokines in Osteoblasts J Bone Miner Res;19:2065–2077.

**FIGURE LEGENDS**

**Fig. 1.** HG prevents the pro-survival effect of FF on osteocytic MLO-Y4cells.

MLO-Y4 cells were exposed to normal glucose (NG), HG or L-glucose (25 mM) -osmotic control- for 24h before pulsatile (8 Hz) FF stimulation (10 dynes/cm$^2$) for 10minwas carried out. Static control (SC) corresponds to non-mechanically stimulated cells. **(A)** p-GSK3β, total and nuclear β-catenin,and **(B)** total p-ERK and nuclear ERK protein levels were evaluated by Western blotting in cell and nuclear extracts. Representative autoradiograms are shown. The dividing lines indicate different parts of the same gel (**A**).**(C)**MLO-Y4-nGFP cells were exposed to 50 μM etoposide after FF (or under SC) for 6 h, and subsequently apoptosis was assessed by enumerating nGFP-positive MLO-Y4 cells exhibiting chromatin condensation, and the percentage of apoptotic cells (left panel) or the Δ between percentage of apoptotic cells under HG and NG exposure (right panel), were shown. Apoptosis (mean ± SD) represented 3.6 ± 1.3 %in etoposide-untreated cells. Values correspond to mean ± SD of at least 3 independent experiments in duplicate.*p<0.05; **p<0.01 vs NG-SC value; $^{\#}$p<0.01 vs NG-FF value.

**Fig. 2.**HG prevents the pro-survival effect of FF on osteoblasticMC3T3-E1 cells.

MC3T3-E1 cells were exposed to NG, HG (25mM) or L-glucose for 24h before FF stimulation (10 dynes/cm2) for 10min, or static control (SC). (**A**) p-GSK3β, β-catenin, and (**B**) p-ERK protein levels were evaluated by Western blotting in total protein extracts obtained immediately after the FF. (**C**) To evaluate cell death, MC3T3-E1 cells were exposed to 50 μM etoposide right after the FF or the SC, for 6 h, and subsequently trypan blue exclusion was determined. Values correspond to mean ± SD of 3 independent experiments in duplicate. *p<0.05; **p<0.01 vs NG SC value; #p<0.01 vs NG FF value.

**Fig. 3.**HG or FF pre-treatment inhibited osteoclast precursor migration induced by the CM from MLO-Y4cells but not from MC3T3-E1 cells.

The conditioned medium (CM) from MLO-Y4 and MC3T3-E1 cells subjected or not (static control, SC) to FFfollowing pre-treatment with HG or normal glucose (NG) for 24 h,was collected 18 h thereafter, as described in the text. **(A, left and B)** RAW 264.7 cell migration was assessed by exposing these cells to the different CMs [or to growth medium alone (Co)] for 6 h, using Costar transwellcell culture chamber inserts (8 μm pore size),or a wound healing assay (**A, right),** as described in the text. Representative images are shown in each case. Values correspond to mean ± SD of 3 independent experiments in triplicate. **p<0.01 vsNG-SC-CM value.

**Fig. 4.** Both HG and FF induce changes in chemokinesecretion by MLO-Y4 cells.

MLO-Y4 cells were subjected or not (static control, SC) to FF following pre-treatment with HG or normal glucose (NG) for 24 h, and the cell-conditioned medium (CM) was collected 18h thereafterto determine the following chemokines by Luminex multiplex assay: VEGF, RANTES, MIP-1a, MIP-1b, MCP-1 and GM-CSF. Values correspond to mean ± SD of 3 independent experiments in triplicate. *p<0.05 vs NG-SC value; $^{\#}$p<0.05 vs NG-FF value.

**Fig. 5.** HG and FF pre-treatment differentially affect osteoclast precursor proliferation, differentiation and activity induced by theMLO-Y4 cell-conditioned medium.

RAW 264.7 cells were exposed to the MLO-Y4 conditioned medium (CM) [or not (Co)] following HG exposure and/or FF stimulation, for 14 d, as described in the text. A) RAW 264.7 cell viability was determined by propidium iodide exclusion using flow cytometry, and (B)proliferation was assayed by flow cytometry as described in the text. Values correspond to mean ± SD of 3 independent experiments in triplicate. (C) RAW 264.7 cells were exposed to the different MLO-Y4 CMs supplemented with 40 ng/ml of RANKL and 25 ng/ml of M-CSFto stimulate osteoclast differentiation for 14 d. Osteoclast differentiation (upper panel) was observed by confocal microscopy (giant cells with actin ring and at least 3 nuclei) and osteoclast activity as formation of resorption lacunae detected by SEM (lower panel) was assessed by culturing RAW264.7 cells on hydroxyapatite disksin different experimental conditions for 14 d.

Scale bars = 20µm. (D)size of the resorption cavities in each experimental group was represented *p<0.01 vs Co value; **p<0.01 vs Co value.# p<0.01 vs NG-SC; ## p<0.05 NG-SC.

**Fig. 6.** HG and FF differentially affect RANKL and IL-6 secretion in MLO-Y4 cells.

RANKL (**A**) and IL-6 (**B**) in the MLO-Y4-CMwere analyzed by ELISA as described in Materials and Methods. Values correspond to mean ± SD of 3 independent experiments in triplicate. *p<0.05; **<0.01vs all the other experimental conditionsin each case.

# Figure 1

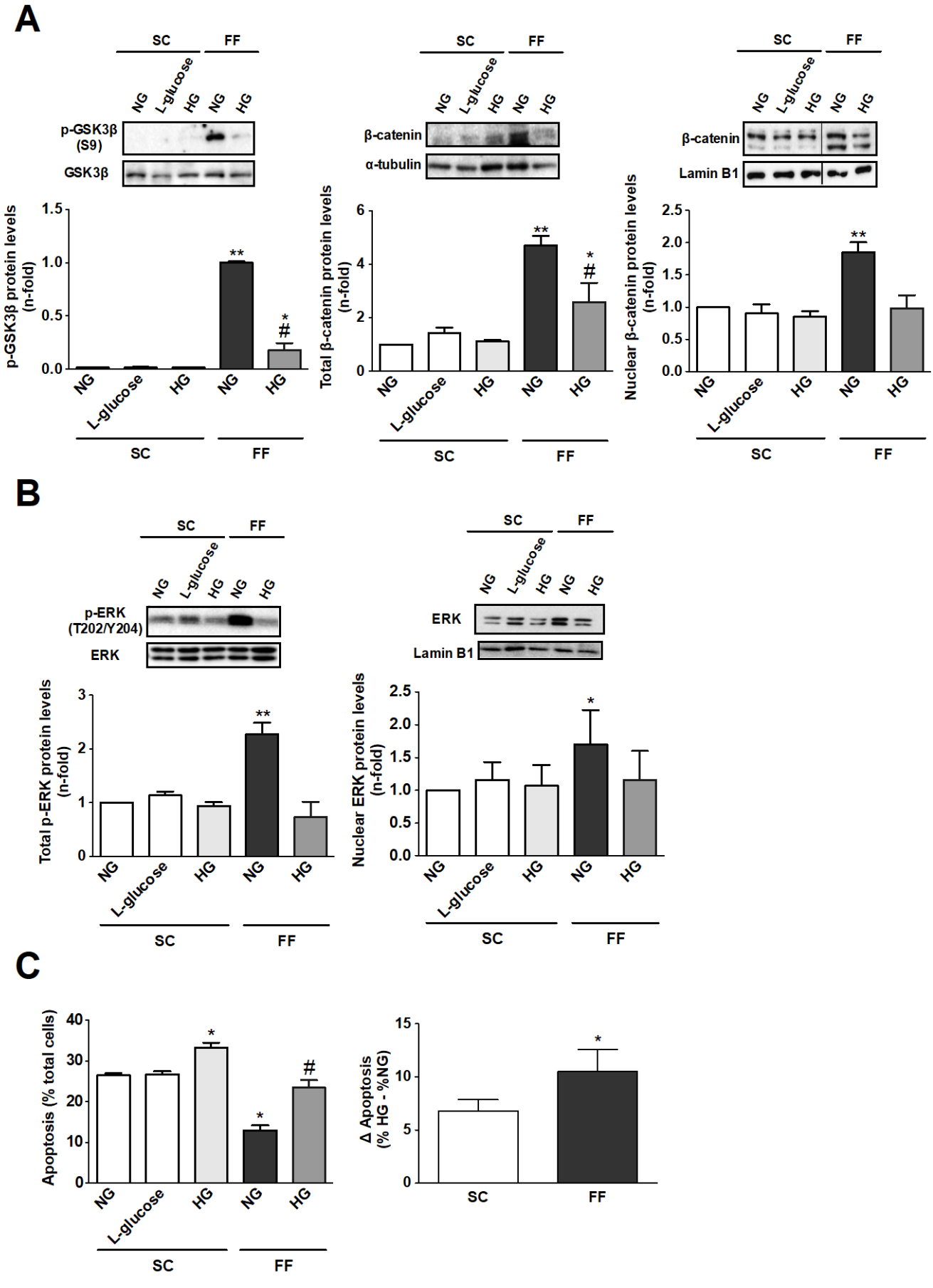
A
SC
FF
NG
L-glucose
HG
p-GSK3β (S9)
GSK3β
p-GSK3β protein levels (n-fold)
β-catenin
α-tubulin
Total β-catenin protein levels (n-fold)
Lamin B1
Nuclear β-catenin protein levels (n-fold)
B
p-ERK (T202/Y204)
ERK
Total p-ERK protein levels (n-fold)
Nuclear ERK protein levels (n-fold)
C
Apoptosis (% total cells)
Δ Apoptosis (% HG - %NG)

# Figure 2

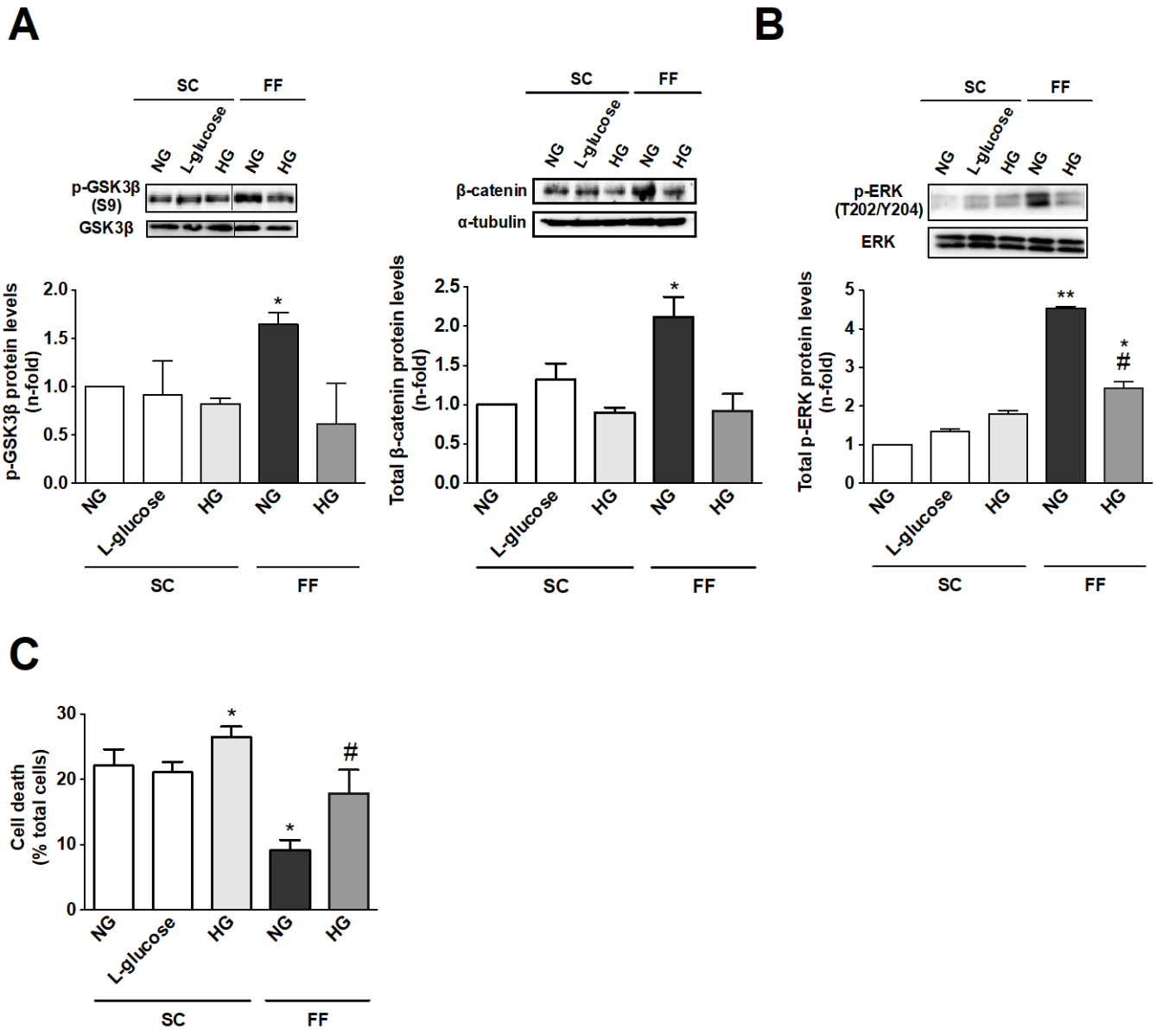
A
B
C
SC
FF
NG
L-glucose
HG
p-GSK3β (S9)
GSK3β
β-catenin
α-tubulin
p-ERK (T202/Y204)
ERK
p-GSK3β protein levels (n-fold)
Total β-catenin protein levels (n-fold)
Total p-ERK protein levels (n-fold)
Cell death (% total cells)

Figure 3

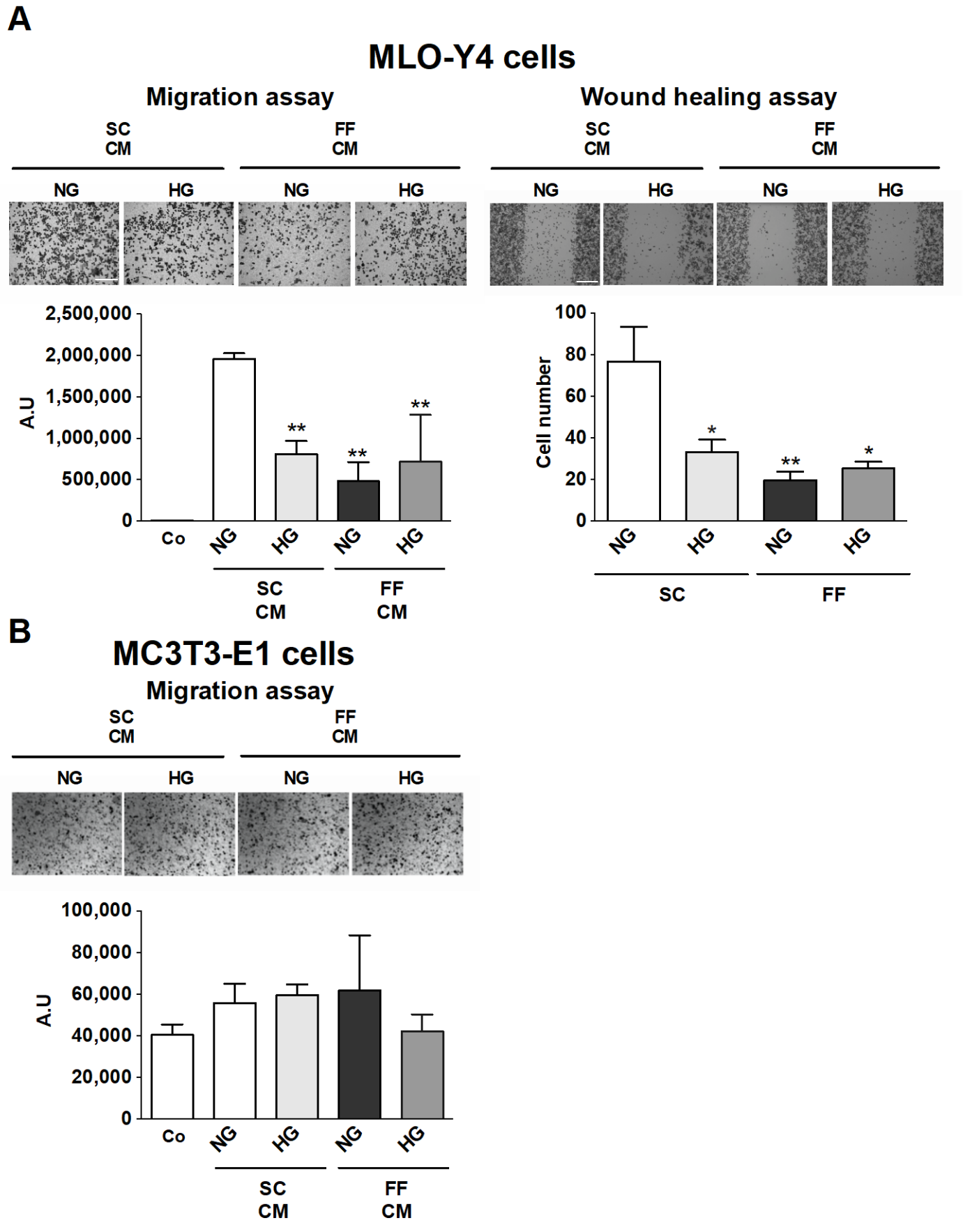
A
MLO-Y4 cells
Migration assay
Wound healing assay
SC CM
FF CM
NG
HG
A.U
Cell number
Co
SC
FF
B
MC3T3-E1 cells
Migration assay

# Figure 4

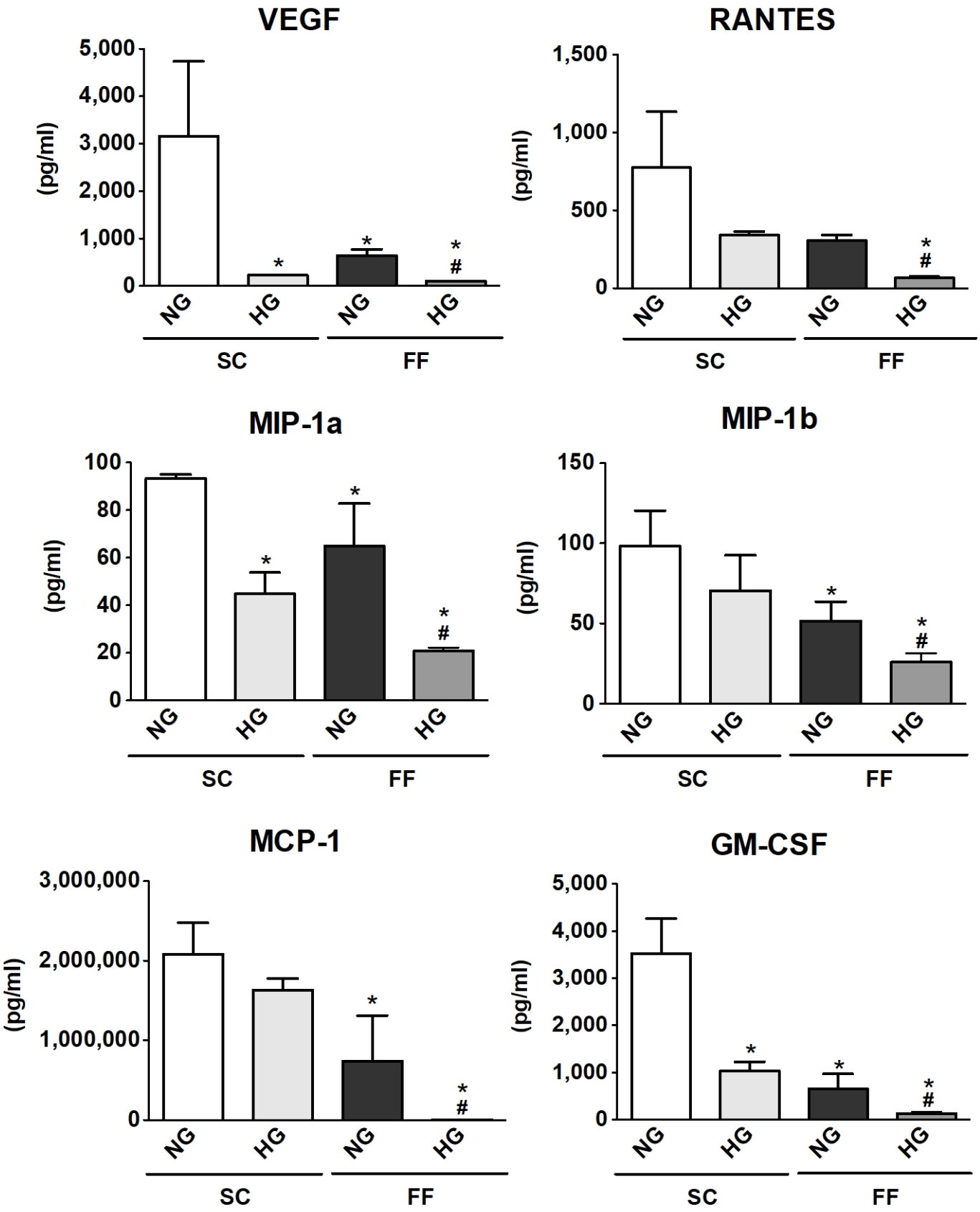
VEGF
5,000
4,000
3,000
2,000
1,000
0
(pg/ml)
*
*
*#
NG
HG
NG
HG
SC
FF
RANTES
1,500
1,000
500
0
(pg/ml)
*#
NG
HG
NG
HG
SC
FF
MIP-1a
100
80
60
40
20
0
(pg/ml)
*
*
*#
NG
HG
NG
HG
SC
FF
MIP-1b
150
100
50
0
(pg/ml)
*
*#
NG
HG
NG
HG
SC
FF
MCP-1
3,000,000
2,000,000
1,000,000
0
(pg/ml)
*
*#
NG
HG
NG
HG
SC
FF
GM-CSF
5,000
4,000
3,000
2,000
1,000
0
(pg/ml)
*
*
*#
NG
HG
NG
HG
SC
FF

# Figure 5

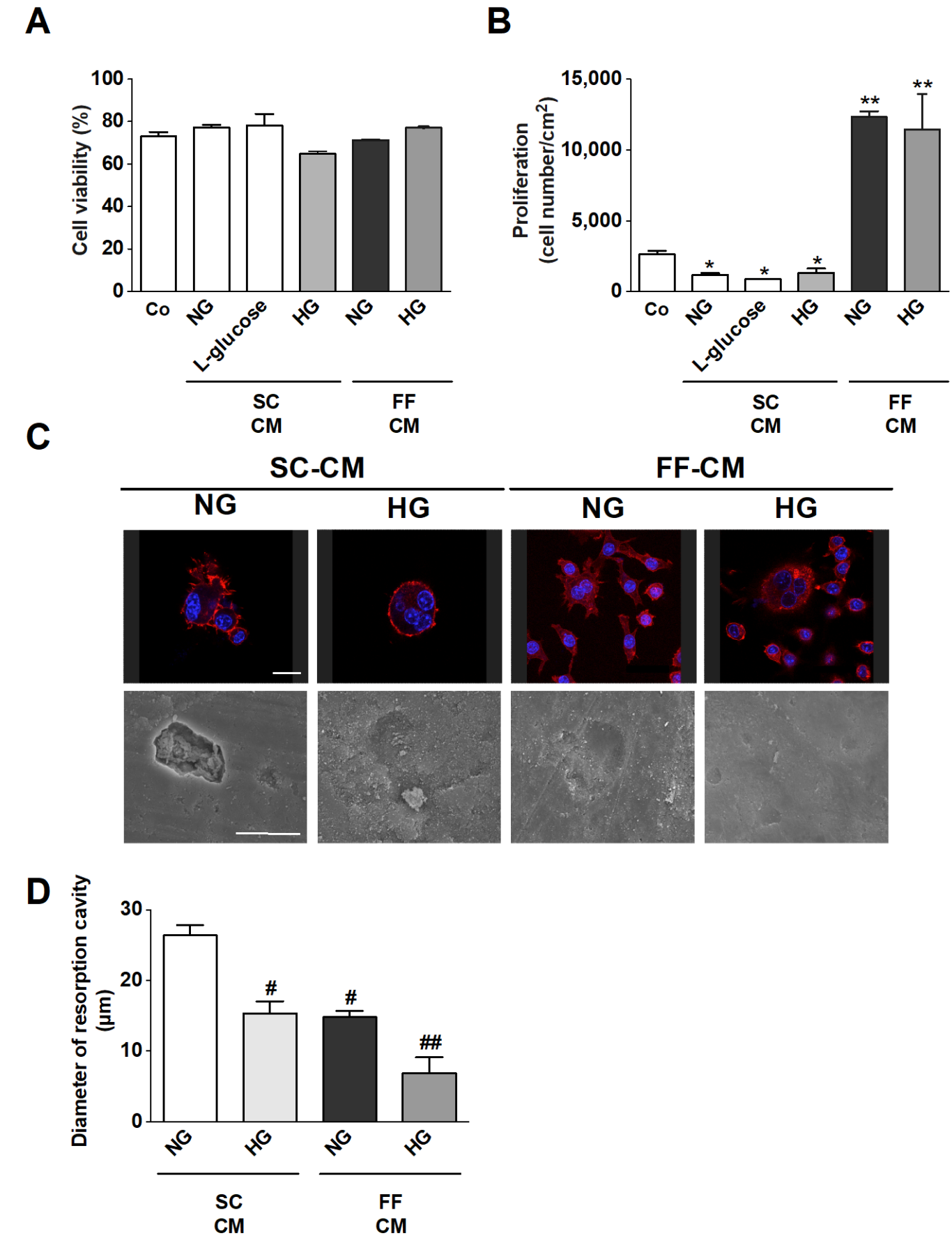
A
Cell viability (%)
100
80
60
40
20
0
Co
NG
L-glucose
HG
NG
HG
SC CM
FF CM
B
Proliferation (cell number/cm2)
15,000
10,000
5,000
0
*
*
*
**
**
Co
NG
L-glucose
HG
NG
HG
SC CM
FF CM
C
SC-CM
FF-CM
NG
HG
NG
HG
D
Diameter of resorption cavity (μm)
30
20
10
0
#
#
##
NG
HG
NG
HG
SC CM
FF CM

# Figure 6

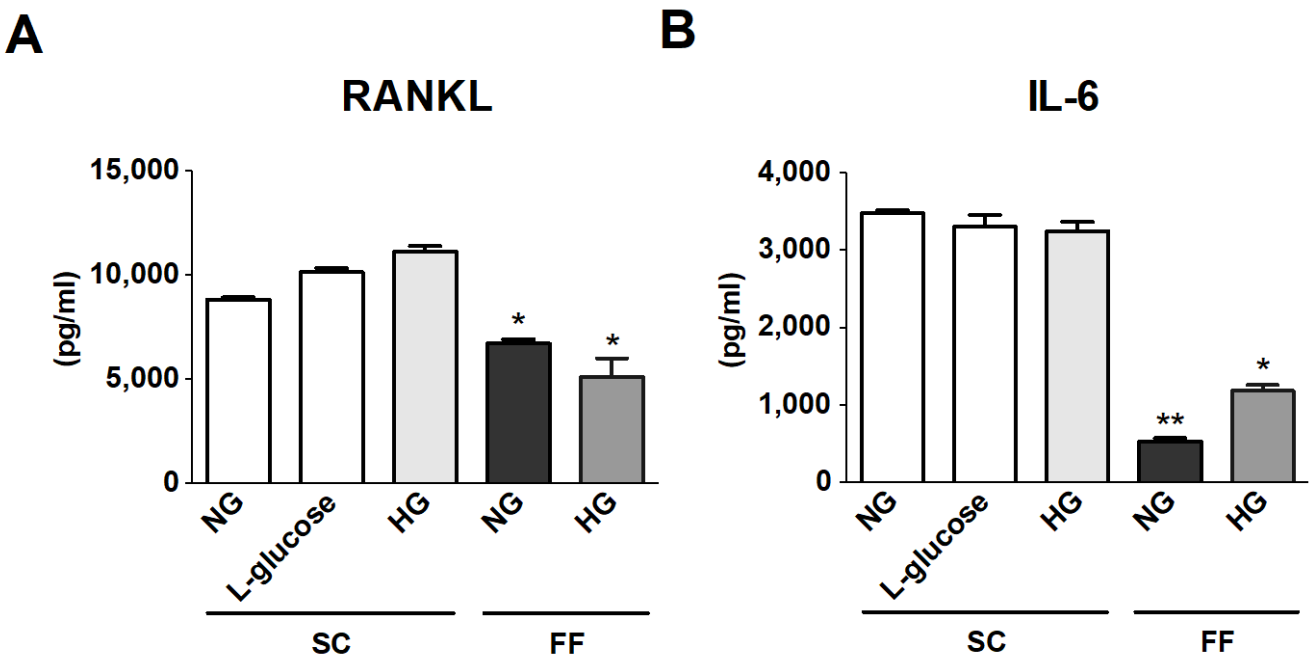
A
RANKL
15,000
10,000
5,000
0
(pg/ml)
*
*
NG
L-glucose
HG
NG
HG
SC
FF
B
IL-6
4,000
3,000
2,000
1,000
0
(pg/ml)
**
*
NG
L-glucose
HG
NG
HG
SC
FF